15 December 1999

ELSEVIER

Optics Communications 172 (1999) 211–227

OPTICS COMMUNICATIONS

www.elsevier.com/locate/optcom

Full length article

# A comparison between lumped and distributed filter models in wavelength-division multiplexed soliton systems

Mark J. Ablowitz, Gino Biondini *, Sarbarish Chakravarty, Rudy Horne

*Department of Applied Mathematics, University of Colorado at Boulder, Campus Box 526, Boulder, CO 80309-0526, USA*

Received 19 August 1999; accepted 5 October 1999

**Abstract**

The effects of lumped and distributed filtering on soliton interactions are considered in a dispersion-managed transmission link when the dispersion steps approximate the loss/amplification profile. A detailed comparison of the collision-induced timing shifts and corresponding timing jitter for both lumped and distributed filtering models is carried out. In particular, we show that: (i) there are some differences between the predictions obtained by the two models; however, (ii) in all cases of practical interest (i.e., non-negligible bit error rates) the estimates originating from the distributed model represent a good approximation to the results obtained with the lumped model. 

*PACS:* 42.97.S; 22.65.Tg; 42.81.Dp
*Keywords:* Fiber optics; Solitons; Wavelength-division multiplexing

## 1. Introduction

The increased demand for communication systems with capacities of several hundreds of gigabit/s and higher has stimulated additional research on solitons as possible carriers of information in long distance transmission links in the last few years (see e.g. Refs. [1,2] and references therein). Essential ingredients to attain such ultra-high capacities are wavelength-division multiplexing, dispersion management and filtering.

One of the major issues in the implementation of wavelength-division multiplexed (WDM) soliton transmission lines over transoceanic distances is to understand the factors limiting the total throughput of the system. In particular, random shifts in pulse arrival times due to nonuniform pulse interactions in a real fiber are known to cause serious penalties in multi-channel systems (see e.g. Refs. [3,4]), and many studies have been subsequently devoted to this subject. It is also well-known that the use of filters and dispersion management can provide a significant reduction in collision-induced timing jitter (see e.g. Refs. [5–23] and references therein).

At the present time, two different ways are known to implement dispersion management. The first approach, which is the most commonly used, is to periodically compensate for the dispersion accumulated by the pulse during propagation through a given distance [24,25]. A second approach is to use subdivide each amplification span into a number of

* Corresponding author. Tel: (303)492-6974; fax: (303)492-4066; e-mail: biondini@colorado.edu

0030-4018/99/$ - see front matter 
PII: S0030-4018(99)00605-7

segments so that the variation of the fiber dispersion in the whole span approximates the variation of the pulse peak power due to fiber absorption [26]. We refer to this second type of dispersion management as 'dispersion management following the loss profile'. It is interesting to note that, although less widely studied, dispersion management following the loss also has the potential for ultra-high transmission rates. Indeed, experiments using filters and this type of dispersion management have demonstrated soliton WDM transmission at 70 Gbit/s over 9000 km with 7 channels at 10 Gbit/s per channel [27], and, more recently, 160 Gbit/s with 8 channels at 20 Gbit/s per channel over 10000 km [28].

In most classical studies of filtering effects on soliton transmission links (see e.g. Refs. [6–14]), it has been standard practice to approximate the filter transfer function by a continuous equivalent distributed along the fiber. We refer to this approach the 'distributed' filtering model. Recently, a filter model was introduced in Ref. [5] which takes into account the discrete positioning of the filters along the system. We will call this approach the 'lumped' filtering model. In Ref. [5] it was argued that the real action of the filters may differ from that described by the distributed model in the case when the characteristic length of the soliton interactions is so short that no filters are encountered during a collision. It was also suggested that a further distinction between the two models arises when the dispersion profile exactly compensates the fiber loss. Namely, the lumped filtering model predicts a non-vanishing residual timing shift after a two soliton collision, whereas previous results indicate that the distributed model yields no timing shift.

In order to accurately model the behavior of long distance transmission lines, it is essential to understand how well the distributed filtering model represents the real action of filters. In this article we present a comparison between the results obtained using the lumped filtering model and the more traditional distributed approximation in the case where the lumped filters are located at the amplifier positions. For simplicity of treatment, we restrict ourselves to the case of dispersion management following the loss profile. However, we emphasize that the methods presented here can be applied, with due modifications, to the situation where the fiber dispersion changes sign within a dispersion map, and that this type of comparison remains relevant in that scenario. In fact, even though the usually low values of average dispersion imply a rather large total collision length (which means that a sizeable number of filters are going to be encountered during the collision), pulse interactions in strongly dispersion-managed systems are characterized by multiple collisions, each of which happens within a length which is inversely proportional to the local values of the dispersion, which can be very high. This means that, in each of the individual collisions, few or no filters are encountered.

The structure of this work is the following. In Section 2, using an analytical approach based on soliton perturbation theory, we calculate the collision induced timing shifts for both lumped and distributed filtering models. Detailed derivations of the timing shifts for each model are included in Appendices B and C. In Section 3, we apply the statistical analysis introduced in Refs. [6,4], to estimate the RMS jitter in pulse arrival times. Also, we compare our results for the two models in the case of stepwise dispersion management with 2-step, 3-step and 4-step dispersion maps. In particular we show that while there are differences between the two models, in the cases of physical interest (i.e., non-negligible bit error rates) the estimates from the continuous approach are a good approximation to those produced by the lumped model. As a limiting scenario, we consider the case when the dispersion profile exactly compensates the fiber loss. In this case, our analysis indicates that there is still a residual timing jitter even for the distributed filter model, contrary to what is commonly believed. We then provide an estimate of this timing shift for standard values of system parameters, and compare it with the corresponding lumped model. Finally, in Section 4, we extend our estimates for two-soliton interactions to a multi-channel WDM transmission system by assuming pairwise collisions between the channels. Again, we find that the system performance predicted by the two models are close.

To our knowledge, this study constitutes the first detailed comparison between the distributed and lumped filtering models and as such it provides the first test of the validity of the distributed filtering approach in studies of wavelength-division multiplexed soliton systems.

## 2. Timing jitter in two-soliton interactions

In this section we review some fundamental results relative to wavelength-division multiplexed soliton propagation and we derive the basic formulae which we use to compute the collision-induced timing shifts in both types of filtering models.

### 2.1. Pulse propagation

Our starting point is the well-known propagation equation for the rescaled dimensionless optical pulse amplitude $u$, i.e. the perturbed nonlinear Schrödinger equation (NLS) with damping/amplification, filtering and dispersion management:

$$iu_z + D(z)\,u_{tt}/2 + g(z)|u|^2 u = iF[t]\,u. \qquad (1)$$

The variables $z$ and $t$ are the usual non-dimensional space and retarded time, normalized to the dispersion length $z_* = 2\pi c t_*^2/(\lambda^2 \overline{D})$ and the characteristic time $t_* = \tau/1.763$, respectively, where $\lambda = 1.550\,\mu$m is the central wavelength, $\overline{D}$ is the path-averaged dispersion parameter, $\tau$ is the full width at half maximum intensity and $c$ is the speed of light in vacuum. Throughout this work we use the typical values $\tau = 20$ ps and $\overline{D} = 0.5\,\text{ps}/(\text{nm}\cdot\text{km})$, which yield $t_* = 11.35$ ps and $z_* = 201.9$ km. The function $g(z)$ describes the periodic energy gain/loss profile:

$$g(z) = a_0^2 \exp\left[-2\Gamma(z - nz_a)\right],$$
$$nz_a \le z < (n+1)z_a;\ n \in \mathscr{Z}. \qquad (2)$$

Here $\Gamma = \gamma z_* = 4.645$ is the dimensionless damping coefficient which corresponds to 0.2 dB/km in physical units; $z_a = l_a/z_*$ is the dimensionless amplifier spacing, and $l_a = 25$ km is the amplifier length that will be used throughout this paper and $a_0^2 = 2\Gamma z_a/[1 - \exp(-2\Gamma z_a)]$. The function $D(z)$ describes the particular choice of dispersion management.

In this article we consider the case $D(z) > 0$ and we study dispersion management following the loss profile; that is, $D(z)$ is taken to approximate the energy profile of the pulse in the fiber due to damping and amplification. Also, we normalize $D(z)$ such that it averages to unity over an amplification period. The change of variable $\zeta(z) = \int_0^z D(z')dz'$, transforms Eq. (1) into

$$iu_\zeta + u_{tt}/2 + G(z)|u|^2 u = i(F[t]/D(z))\,u, \qquad (3)$$

where $G(z) = g(z)/D(z)$.

The term $F[t]$ in Eq. (1) represents the contribution due to filters. Namely,

$$F[t]_{\text{lumped}} = \left[\eta_0 - \eta_2(i\partial_t - \omega_f)^2\right] z_f \times \sum_{n=-\infty}^{\infty} \delta(z - nz_f) \qquad (4a)$$

for the lumped model, and

$$F[t]_{\text{distributed}} = \eta_0 - \eta_2(i\partial_t - \omega_f)^2 \qquad (4b)$$

for the distributed model (see Appendix A), where $\eta_2$ is the filter strength, $\eta_0$ is the additional gain required to overcome the energy loss due to filters and $z_f$ is the filter spacing. As is commonly done, we will consider the filters to be positioned at amplifier locations, i.e. we set $z_f = z_a$.

### 2.2. Collision-induced frequency shifts

We calculate the timing shifts resulting from a single two-soliton collision in the physically important case when the soliton channels are widely separated in the frequency domain. Similar to the ideal case (cf. [29,30]), we decompose $u$ to leading order as $u(\zeta,t) \sim u_1(\zeta,t) + u_2(\zeta,t)$, where

$$u_j = A_j \operatorname{sech} A_j\left[t - \Omega_j(\zeta - \zeta_o)\right] \times \exp i\left[\Omega_j t - \left(\Omega_j^2 - A_j^2\right)\zeta/2\right], \qquad (5)$$

where $\zeta_o = \zeta(z_o)$ is the collision point, and where, as an effect of the perturbations, $A_j$ and $\Omega_j$ are slowly varying with respect to $z$. Dropping terms which are $O(z_a, 1/\delta\Omega)$ (where $\delta\Omega = \Omega_2 - \Omega_1$), $A_j$ can be taken to be a constant, which we normalize to unity. We choose the unperturbed frequencies as $\Omega_2 = -\Omega_1 =: \Omega > 0$. Soliton perturbation theory then allows us to calculate the slow variation of the soliton mean frequencies $\pm\Omega$. For the pulse with mean frequency $\Omega$, we obtain

$$\frac{d\Omega}{dz} = G(z)\frac{d}{dz}\left[f(\zeta(z) - \zeta_o)\right] - (4/3)\eta_2(z)(\Omega - \omega_f), \qquad (6)$$

where $f(z) = \int_{-\infty}^{\infty} \mathrm{sech}^2(t - \Omega z)\mathrm{sech}^2(t + \Omega z)dt$ expresses the frequency shift in the ideal ($D(z) = g(z) = 1$) case, and $\Omega(-\infty) = \omega_f$. Explicitly, $f(z) = (2/\Omega)[2\Omega z\cosh(2\Omega z) - \sinh(2\Omega z)]\mathrm{csch}^3(2\Omega z)$ (cf. Ref. [3]). Recall that for the distributed model $\eta_2(z) \equiv \eta_2$, while for the lumped model $\eta_2(z) = \eta_2 z_f \sum_{n=-\infty}^{\infty} \delta(z - nz_f)$ (cf. Appendix A). Treating the first term in the right hand side as a forcing we can integrate Eq. (6) exactly to obtain the frequency shift $\Delta\Omega(z) = \Omega(z) - \Omega(-\infty)$:

$$\Delta\Omega(z) = \int_{-\infty}^{z} \exp[H(z') - H(z)] \times G(z') \frac{d}{dz'} f(\zeta(z') - \zeta_0)\, dz', \qquad (7)$$

where the frequency shift $\Delta\Omega(z) = \Omega(z) - \Omega(-\infty)$. For the distributed model

$$H(z) = (4/3)\eta_2 z$$

and, for the lumped model

$$H(z) = (4/3)\int_{0^+}^{z} \eta(z')\, dz' = (4/3)\eta_2 \lfloor z/z_a \rfloor,$$

where the 'floor' function is defined as $\lfloor x \rfloor = n$, $n \le x < n + 1$; $n \in \mathscr{Z}$. A more convenient representation is

$$H(z) = (4/3)\eta_2 (z - s(z)),$$

where $s(z)$ is the periodic extension of $s(z) = z$, $0 \le z < z_a$.

### 2.3. Collision-induced timing shifts

The solitons experience a phase shift due to collisions cause a jitter in the pulse arrival time. If the pulse evolution is governed by Eq. (5), the mean time position

$$\langle t \rangle = \int_{-\infty}^{\infty} t\,|u_j|^2\, dt \Big/ \int_{-\infty}^{\infty} |u_j|^2\, dt$$

satisfies $d\langle t \rangle/dz = \Omega_j(z)D(z)$. The collision-induced shift in the mean position of the (faster) pulse $u_1$ at a location $L$ far along the fiber, will be:

$$\delta t = -\int_{-\infty}^{L} \Delta\Omega(z(\zeta))\, d\zeta = -\int_{-\infty}^{L} \Delta\Omega(z) D(z)\, dz. \qquad (8)$$

(The minus sign is due to the mean frequency of $u_1$ being $-\Omega$.) Physically, the presence of $D(z)$ in Eq. (8) means that the change in the (inverse) group velocity of the pulse is the product of the frequency shift and local dispersion. In the constant dispersion case $D(z) = \overline{D} = 1$. Since $D(z)$ averages to unity, we can express $D(z) = 1 + \Delta(z)$ where $\Delta(z)$ represents the rapid periodic, zero-mean oscillations of the fiber dispersion around its mean value. The timing jitter in Eq. (8) can then be decomposed as

$$\delta t = -\left[\int_{-\infty}^{L} \Delta\Omega(z)\, dz + \int_{-\infty}^{L} \Delta\Omega(z)\,\Delta(z)\, dz)\right]. \qquad (9)$$

The first term in Eq. (9) is the contribution from path averaged dispersion toward the total collision-induced timing shift, while the second term originates from the local variation of dispersion in the fiber. In the case of dispersion management following the loss profile (where $D(z)$ has period $z_a$), the contribution of the second term in Eq. (9) is only $O(z_a)$ (see Appendix C) and does not significantly affect the overall timing jitter if $z_a \ll 1$.

Substituting Eq. (7) into Eq. (8) and interchanging the order of integration, we obtain the asymptotic timing shift in the limit $L \to \infty$:

$$\delta t = -\int_{-\infty}^{\infty} a(z)G(z)\frac{d}{dz} f(\zeta(z) - \zeta_0)\, dz, \qquad (10a)$$

where

$$a(z) = \int_{z}^{\infty} \exp[H(z) - H(z')]\, D(z')\, dz'. \qquad (10b)$$

Expanding $G(z(\zeta))a(z(\zeta))$ in Fourier series and computing the resulting integrals, we find

$$\delta t = -\sum_{m=1}^{\infty} |p_m| c_m \sin[2m\pi\zeta_0/z_a + \arg(p_m)], \qquad (11)$$

where $c_m(\Omega) = \int_{-\infty}^{\infty} e^{im z/z_a}(d/dz)[f(\zeta(z) - \zeta_0)]dz$, the $p_m$ are the Fourier coefficients of $G(z(\zeta))a(z(\zeta))$ and $G_m$ and $S_m$ are the Fourier coefficients of $G(z(\zeta))$ and $s(\zeta)G(z(\zeta))$, respectively. Explicitly,

$$c_m(\Omega) = \pi^5 m^3/\Omega^4 z_a^3 \sinh^2\left(m\pi^2/2\Omega z_a\right), \qquad (12)$$

while the $p_m$ are given by

$$p_m = (3/4\eta_2)\,\hat{G}_m \tag{13a}$$

for the distributed model, and

$$p_m = z_a G_m/(1-\exp[-4\eta_2 z_a/3]) - (iz_a/2\pi)\,S_m\,. \tag{13b}$$

for the lumped model. Detailed derivations of Eq. (11) for both models are given in Appendices B and C. Note that if $z_f \neq z_a$ but $z_f/z_a$ is rational, then the Fourier coefficients $p_m$ for the lumped model in Eq. (13b) are calculated over the smallest common period of $z_f$ and $z_a$. The Fourier coefficients $G_m$, $\hat{G}_m$ and $S_m$ depend on the specific choice of dispersion $D(z)$. As mentioned in Section 1, we consider $D(z)$ to be a stepwise approximation to the ideal exponential shape. To this purpose, we divide the amplification period into $S$ spans with endpoints $z_0, z_1, \ldots, z_S$ (with $z_0 = 0$ and $z_S = z_a$), and take $D(z) = D_s$ for $z_{s-1} \le z < z_s$, where $D_s$ is obtained by requiring that $G(z)$ averages to unity in each of the sub-intervals (cf. [15]). The last condition amounts to

$$D_s = \frac{a_0^2}{z_s - z_{s-1}} \int_{z_{s-1}}^{z_s} \exp[-2\Gamma z]\,dz = a_0^2\,\frac{\exp[-2\Gamma z_{s-1}] - \exp[-2\Gamma z_s]}{2\Gamma(z_s - z_{s-1})}\,. \tag{14}$$

Then by integrating piecewise over each span $z_{s-1} \le z < z_s$ with constant dispersion coefficient $D_s$, the $G_m$ are given by

$$G_m = (1/z_a)\int_0^{z_a} G(z(\zeta))\exp[-2m\pi i\zeta/z_a]\,d\zeta = \sum_{s=1}^{S} G_{m.s}\,, \tag{15}$$

where $G_{m,s} = q_{m,s}/(2\Gamma z_a - 2m\pi i D_s)$ with

$$q_{m,s} = \exp[-(2\Gamma z_{s-1} - im\kappa_{s-1})] - \exp[-(2\Gamma z_s - im\kappa_s)]\,,$$

$$\kappa_s = (2\pi/z_a)\int_0^{z_s} D(z)\,dz$$

and $D_s$ follows from Eq. (14). The coefficients $\hat{G}_m$ differ from the $G_m$ by a small correction factor arising from the second term of Eq. (9), which encapsulates the effect of the local variation of dispersion. The explicit expressions for $\hat{G}_m$ in the case of stepwise dispersion management are rather involved, although straightforward to compute. For this reason, we present them in Appendix C. The derivation of the timing shift for the distributed filter model was given in Ref. [6] where only the dominant contribution (i.e. only the first term of Eq. (9)) was considered. This simplification leads to the convenient approximation $p_m \approx (3/4\eta_2)G_m$ instead of $p_m = (3/4\eta_2)\hat{G}_m$ in Eq. (13a). Here we include the small correction term for a more accurate comparison between the timing jitter in the lumped and distributed models.

## 3. Statistical estimates and comparisons

Once the timing shift induced by a single collision is known, the mean square timing jitter resulting from the large number of collisions that take place over the total length of a two-channel transmission system can be computed.

### 3.1. Statistical properties of the timing shifts

Consider the timing shift of the $n$-th encoded soliton in channel 1 due to interactions with solitons in channel 2. This is given by $b_n \delta t(z_n)$, where $z_n$ is the $n$-th collision point, and $b_n$ is 0 or 1 depending on the data encoding in channel 2. The total timing shift is the sum of the shifts resulting from all the collisions in the system

$$\Delta t = \sum_{n=1}^{N} b_n \delta t(z_n)\,,$$

where $N(\Omega)$ is the total number of collisions occurring within the fiber. Explicitly, $N(\Omega) = (2\Omega)L/T$, where $T = 5\tau/t_*$ is the dimensionless bit period. (Here we assume a separation of five pulse widths

between adjacent pulses.) We treat $b_n$ and $\delta t(z_n)$ as independent random variables and assume that the collision point $z_n$ occurs randomly in an amplifier length. Hence, $\langle \delta t(z_n)\rangle = 0$ and $\langle \delta t(z_m)\delta t(z_n)\rangle = 0, m \neq n$. So the variance of the total timing shift $\Delta t$ due to a large number of independent collisions is

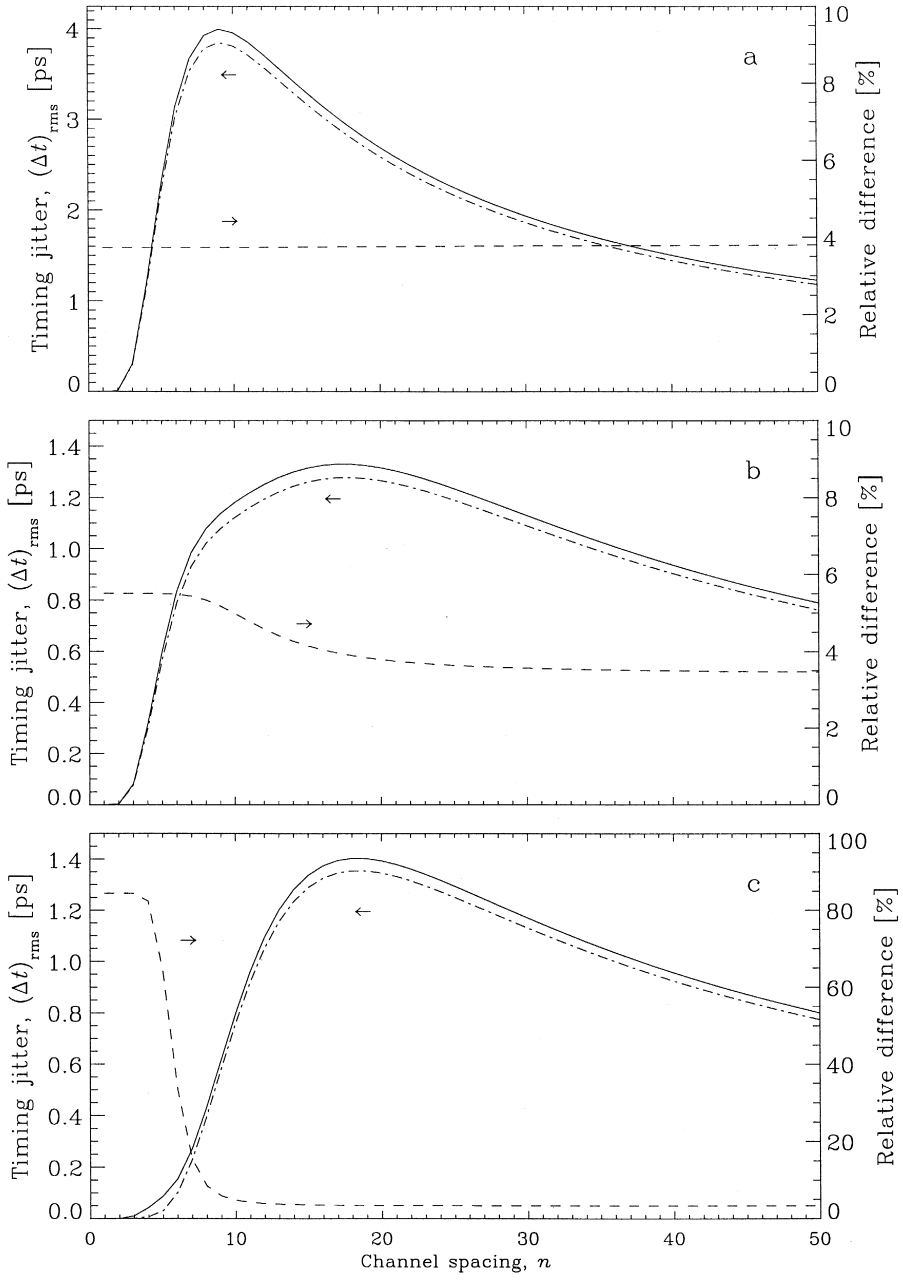


Fig. 1. The root mean square (rms) timing shift $(\Delta t)_{\rm rms}$ at a propagation distance of 10000 km versus channel spacing $(n)$ in a two-channel WDM system with a two-step dispersion map following the loss profile ($\tau = 20$ ps, $\overline{D} = 0.5$ ps/(nm · km), $l_a = 25$ km, $\Gamma = 4.645$ and $\eta_2 = 0.25$): (a) no dispersion management; (b) $\theta = 0.5$; (c) $\theta = 0.416$. Solid curve: lumped filters; dot-dashed curve: distributed filters; dashed curve: relative difference in $(\Delta t)_{\rm rms}$ values between lumped and distributed filters (right scale).

given by the sum of individual variances. Then we can apply the results of the statistical analysis developed in Refs. [6,4] and obtain

$$(\Delta t)^2_{\rm rms} \equiv \langle (\Delta t - \langle \Delta t \rangle)^2 \rangle = \langle (\Delta t)^2 \rangle = (N/4) \sum_{m=1}^{\infty} |p_m|^2 c_m^2 , \qquad (16)$$

with $p_m$ given by either Eq. (13a) or Eq. (13b).

Having constructed the analytical framework to study collision-induced timing jitter with both lumped and distributed filter models, we can now apply the previous formulae in order to compare their respective predictions. Note that the coefficients $p_m$ in Eq. (16) depend on $D(z)$, and therefore on the locations of the intermediate points $z_s$ for a stepwise dispersion map, whereas the coefficients $c_m$ in Eq. (16), are functions only of $z_c/z_a$, where $z_c = \tau/\Omega t_*$ is the dimensionless collision length and $2\Omega$ is the dimensionless frequency separation between the soliton channels. In our case $z_a$ is fixed since we have set the amplifier spacing $l_a = 25$ km, so that $c_m$ vary only with the channel frequency spacing $2\Omega$. From Eq. (14) it follows that for a 2-step map, the only free parameter is the ratio $\theta$ between the intermediate length $z_1$ and the amplification period, $\theta = z_1/z_a$. The dimensionless frequency separation $2\Omega$ is chosen as $n(\Delta\Omega)_{\rm min}$, $n = 1,2,3,\ldots$, where $(\Delta\Omega)_{\rm min} = 5.6$ corresponds to five spectral widths or (with our choice of parameters) a wavelength separation of $(\Delta\lambda)_{\rm min} = 0.63$ nm. For this choice of frequency separation, it is $z_c/z_a = 5.07/n$.

### 3.2. Numerical estimates

Using the analytical formula (13b), we can now estimate the timing jitter in a number of cases.

In Fig. 1 we plot $(\Delta t)_{\rm rms}$ (in ps) corresponding to a total fiber length $L = 10$ Mm as a function of the frequency separation for a two-channel system with a 2-step dispersion map. We display the results for both the lumped model (solid lines) and the distributed model (dot-dashed lines) in the following three situations: (a) no dispersion management; (b) fiber spans of equal length, i.e. $\theta = 0.5$; (c) the value of $\theta$ that minimizes the first Fourier coefficient $|G_1|$ (cf. Ref. [6]), $\theta = 0.416$. The dashed lines represent the relative difference between the lumped and the distributed result. In all three cases both models have essentially similar profiles. We note that their relative difference is $\leq 5\%$ for a wide range of channel

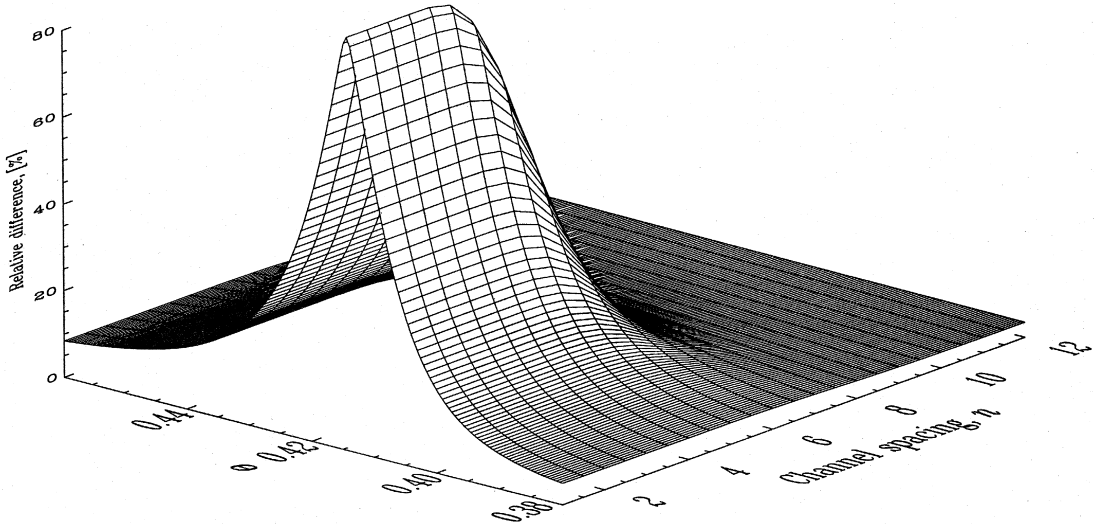


Fig. 2. Relative difference in $(\Delta t)_{\rm rms}$ values at 10000 km between lumped and distributed filters as a function of $\theta$ and frequency separation $n$ with a two-step dispersion map following the loss profile. The values of the system parameters $\tau$, $\bar{D}$, $l_a$, $\Gamma$ and $\eta_2$ are the same as in Fig. 1.

separation. In case c) the relative difference between the two models is large when the timing jitter is relatively small and occurring for frequency separations corresponding to $n \leq 9$ (or $z_c/z_a \geq 0.57$). Mathematically this discrepancy arises mainly from the first Fourier coefficient, i.e. the term $m = 1$ in Eq. (16). This happens because, when $\theta = 0.416$, both $|G_1|$ and $|\hat{G}_1|$ are much smaller than $|S_1|$ (see Eqs. (13a) and (13b)). However, for frequency separations between channels corresponding to $n \leq 9$, the values of $(\Delta t)_{\text{rms}}$ are less than or equal to 0.2 ps for both filtering models (cf. Fig. 1c), and the corresponding bit error rate (BER) is too small to be significant in a practical WDM transmission line. Moreover, with increasing frequency separation the relative difference between the two models rapidly decreases to an almost negligible value ($< 4\%$) as is evident from Fig. 1c. This fact can be also clearly seen from the surface plot in Fig. 2 of the relative difference in $(\Delta t)_{\text{rms}}$ between the two models versus the frequency separation $n$ and the dispersion map parameter $\theta$. Fig. 2 indicates that the large relative difference between the models is not only restricted to values of $n \leq 9$ but also to a very small range of $\theta$ around $\theta = 0.416$.

In Fig. 3, we plot the RMS timing jitter $(\Delta t)_{\text{rms}}$ as a function of $n$ for: (a) 3-step map and (b) 4-step map, both with equal step sizes. In both cases we show the results of: (i) lumped model (solid lines); (ii) distributed model (dot-dashed lines). The dashed lines represent the relative difference between the lumped and the distributed results. Note that, as the

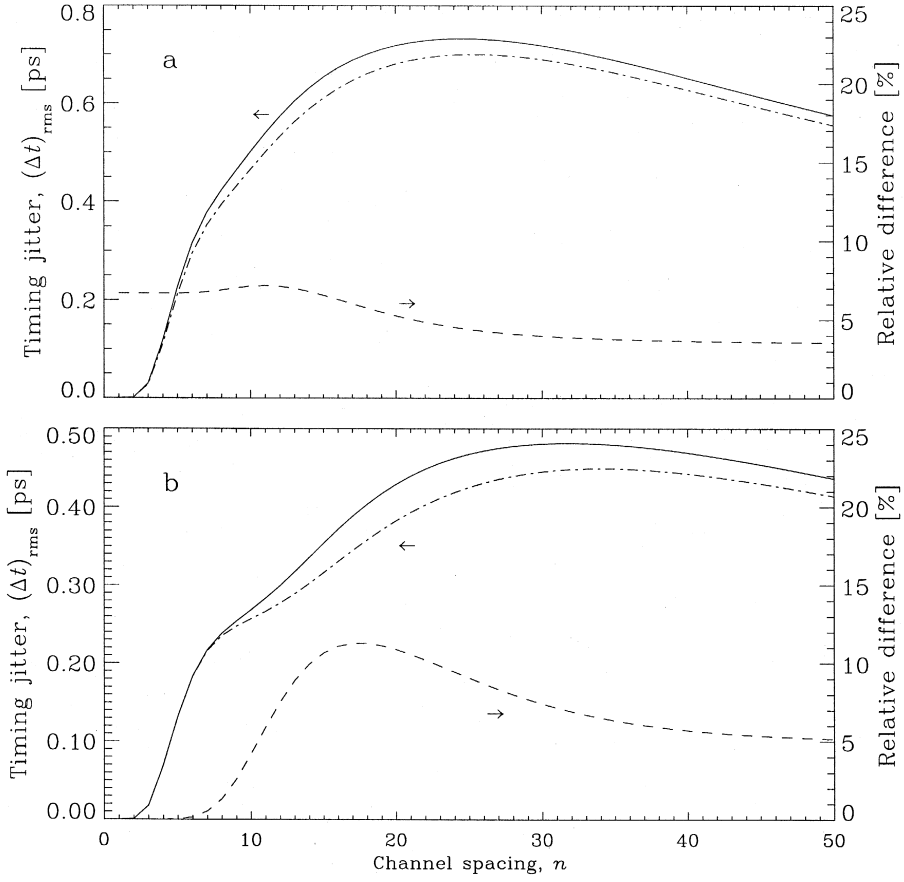


Fig. 3. $(\Delta t)_{\text{rms}}$ at 10000 km in a two-channel system for: (a) 3-step dispersion map; (b) 4-step dispersion map with equal step sizes in both cases. Solid curve: lumped filters; dot-dashed curve: distributed filters; dashed curve: relative difference in $(\Delta t)_{\text{rms}}$ values between lumped and distributed filters (right scale). System parameters are the same as in Fig. 1.

number of steps increases the value of $(\Delta t)_{\rm rms}$ decreases (by roughly a factor of half with each step). The relative differences between the lumped and distributed models for 3-step and 4-step dispersion maps attain maximum values of approximately 7% and 11% respectively. This is a more significant difference as compared to the 2-step equal length case (i.e. $\theta = 0.5$).

### 3.3. Exponentially tapered fibers

Finally, we consider the limiting situation when the fiber dispersion exactly compensates the loss profile; that is, $D(z) = g(z)$. Physically, this scenario corresponds to the case when the number of steps used in the dispersion map becomes large.

If $D(z) = g(z)$, the timing shift for the distributed model can be obtained by following the calculations detailed in Appendix C. We explicitly calculate $a(z)$ given by Eqs. (10) by evaluating the integrals in Eq. (C.1). Using $D(z) = a_0^2 \exp[-2\Gamma z]$, $0 \le z \le z_a$, and periodically extended, we obtain

$$a(z) = \frac{D(z) + 2\Gamma z_a \gamma \exp[4\eta_2 z/3]}{(4/3)\eta_2 + 2\Gamma},$$

where $\gamma = 1/(\exp[4\eta_2 z_a/3] - 1)$. Then, by inverting the relation

$$\zeta(z) = \int_0^z D(z')\, dz' = a_0^2(1 - \exp[-2\Gamma z])/2\Gamma$$

for $0 \le z \le z_a$ and $0 \le \zeta \le z_a$, we find that

$$a(z(\zeta)) = \frac{z_a}{r(p+1)}\left[1 - \frac{r\zeta}{z_a} + \frac{\gamma r}{(1 - r\zeta/z_a)^p}\right], \tag{17}$$

where $r = 1 - \exp[-2\Gamma z_a]$ and $p = 2\eta_2/3\Gamma$. The corresponding timing shift is obtained from Eqs. (10) after using the fact that $G(z) = 1$,

$$\delta t = -\int_{-\infty}^{\infty} a(z)\frac{d}{dz} f(\zeta(z) - \zeta_{\rm o})\, dz$$

$$= -\sum_{m=1}^{\infty} |a_m| c_m \sin\left[2m\pi\zeta_{\rm o}/z_a + \arg(a_m)\right]. \tag{18}$$

Using Eq. (17) the Fourier coefficients $a_m$ of $a(z(\zeta))$ are estimated from an asymptotic series obtained by repeated integration by parts:

$$a_m \sim \frac{\gamma z_a}{(p+1)(2m\pi)^2}\left[b_1 - \frac{ib_2}{2m\pi} + O(2m\pi)^{-2}\right],$$

$m \neq 0$,

where $b_1 = pr[(1-r)^{-(p+1)} - 1]$, $b_2 = p(p+1)r^2[(1-r)^{-(p+2)} - 1]$. It is clear from the above that the timing shift for the distributed filter model *does not* go to zero. This is due to local variation of dispersion in the fiber, even though the dispersion exactly compensates the fiber loss. The collision-induced timing shift does vanish in a fiber with distributed filters where *both* $D(z)$ and $g(z)$ are equal to unity. This can be easily verified from Eqs. (10) by substituting $D(z) = g(z) = 1$. Then the second integral in Eqs. (10) yields $a(z) = 3/4\eta_2$ and consequently, the first integral leads to $\delta t = 0$.

In the case of lumped filters, the timing shift is obtained from Appendix B after setting $G(z) = 1$. The result is

$$\delta t = -\sum_{m=1}^{\infty} |a_m| c_m \sin\left[2m\pi\zeta_{\rm o}/z_a + \arg(a_m)\right], \tag{19}$$

where $a_m = iz_a/2m\pi$ which follows from Eq. (B.5). From Eqs. (16), (18) and (19) (here $p_m = a_m$), and the corresponding expressions for $a_m$ in the lumped and distributed models, we obtain the following estimate for the rms timing jitter

$$(\Delta t_{\rm rms})_{\rm d}/(\Delta t_{\rm rms})_{\rm l} \le \gamma\left(b_1^2 + b_2^2/4\pi^2\right)^{1/2} /2\pi(1+p).$$

Using $\eta_2 = 0.25$ and $\Gamma = 4.645$ as standard parameter values, the above upper bound is found to be less than about 22.5%. In Fig. 4, we plot the RMS timing jitter for a two-channel system obtained from Eqs. (18) and (19) for the distributed and lumped cases, and their ratio as a function of the dimensionless frequency separation. For small frequency separation, the ratio between the lumped and distributed timing jitter is close to the upper bound estimated above and decreases with increased frequency spacing between the channels. Although the results are significantly different for the two models in this

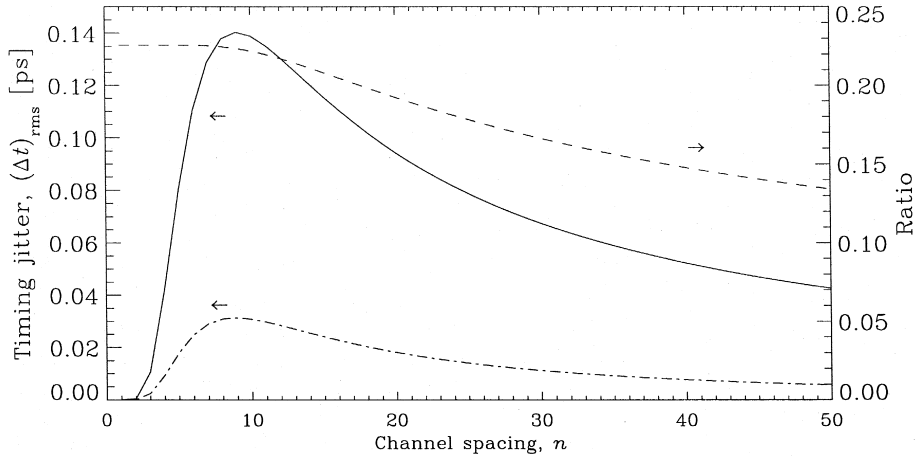


Fig. 4. $(\Delta t)_{\rm rms}$ at 10000 km in a two-channel system when the dispersion exactly compensates the fiber loss/gain profile, i.e. $D(z) = g(z)$. Solid curve: lumped filters; dot-dashed curve: distributed filters; dashed curve: the ratio $(\Delta t_{\rm rms})_{\rm distributed}/(\Delta t_{\rm rms})_{\rm lumped}$ (right scale). Here $\tau$, $\overline{D}$, $l_a$, $\Gamma$ and $\eta_2$ are the same as in Fig. 1.

case, the actual timing jitter values for both models correspond to negligible BER in practical systems.

## 4. Timing jitter in multi-channel systems

In this section we extend the results of Section 3 to WDM systems with more than two channels, and we derive analytical estimates for the behavior of multi-channel systems.

### *4.1. Statistical properties of multi-channel systems*

If we assume that soliton interactions are pairwise to leading order (cf. [4–6] and then the effects of collisions in neighboring channels can be analyzed in a straightforward manner. We can express the total variance in the relative arrival times of adjacent solitons in a given channel $j$ simply as the sum of the variances produced by interactions with all the other channels. The mean square timing jitter for channel $j$ in a system with total number of channels $J$ is

$$(\Delta t)_j^2 = \sum_{\substack{k=1 \\ k\neq j}}^{J} (\Delta t)_{jk}^2 , \qquad (20)$$

where $(\Delta t)_{jk}^2$ is given by Eq. (16) with $c_m = c_m(\Omega_{jk})$, and where $2\Omega_{jk}$ is the frequency separation of channels $j$ and $k$. Given the large number of interactions the values of $\Delta t$ can be reasonably assumed to follow a Gaussian distribution. Then the expected bit error rate (BER) of the system is $\mathrm{BER} = \mathrm{erfc}\,[rT/\sqrt{2}\,(\Delta t)_{\rm rms}]$, where $r$ is defined by assuming that the maximum time displacement tolerated by the receiver is $rT$ and $(\Delta t)_{\rm rms}$ is given by Eq. (20). Clearly, the BER of the system grows with increasing number of channels. In order for the BER of the system to be less than $10^{-9}$ (which we take as the limit for 'error free' transmission) it is necessary that the RMS timing jitter in each of the individual channels be less than $0.164\,rT$. This condition poses an upper limit to the system length for error-free transmission (cf. Ref. [6]):

$$L_{\max} = 36.7\, r^2 / \max_{j=1,\ldots,J} \times \left[ \sum_{\substack{k=1 \\ k\neq j}}^{J} \Omega_{jk} \sum_{m=1}^{\infty} |p_m|^2 c_m^2(\Omega_{jk}) \right]. \qquad (21)$$

($L_{\max}$ in Eq. (21) is non-dimensional; in order to obtain the system length in physical units, $L_{\max}$ should be multiplied by $z_* = 201.9$ km.) For any fixed system length $L_{\max}$, Eq. (21) can also be used to obtain a limit on the number of channels compatible with the desired value of the bit error rate. With the assumption of strictly pairwise interaction between the channels, the outermost channels of the

WDM comb generally suffer the maximum overall timing jitter (cf. Ref. [6]) for the parameter ranges considered in this article. Like in Section 3, we consider the case $L_{\max} = 10\,\text{Mm}$ as the conventional limit distance for transoceanic communications. We choose the channel wavelengths so that the minimum wavelength separation between the adjacent channels is five spectral widths. This corresponds to a dimensionless frequency separation $(\Delta\Omega)_{\min} = 5.6$ between adjacent channels. The dimensionless frequency separation between channels $j$ and $k$ are then given by $2\,\Omega_{jk} = |j-k|\,\Delta\Omega)_{\min}$.

### 4.2. Numerical estimates

In Fig. 5, we plot the net RMS timing jitter (in ps) suffered by the outermost channel $J$ versus the total

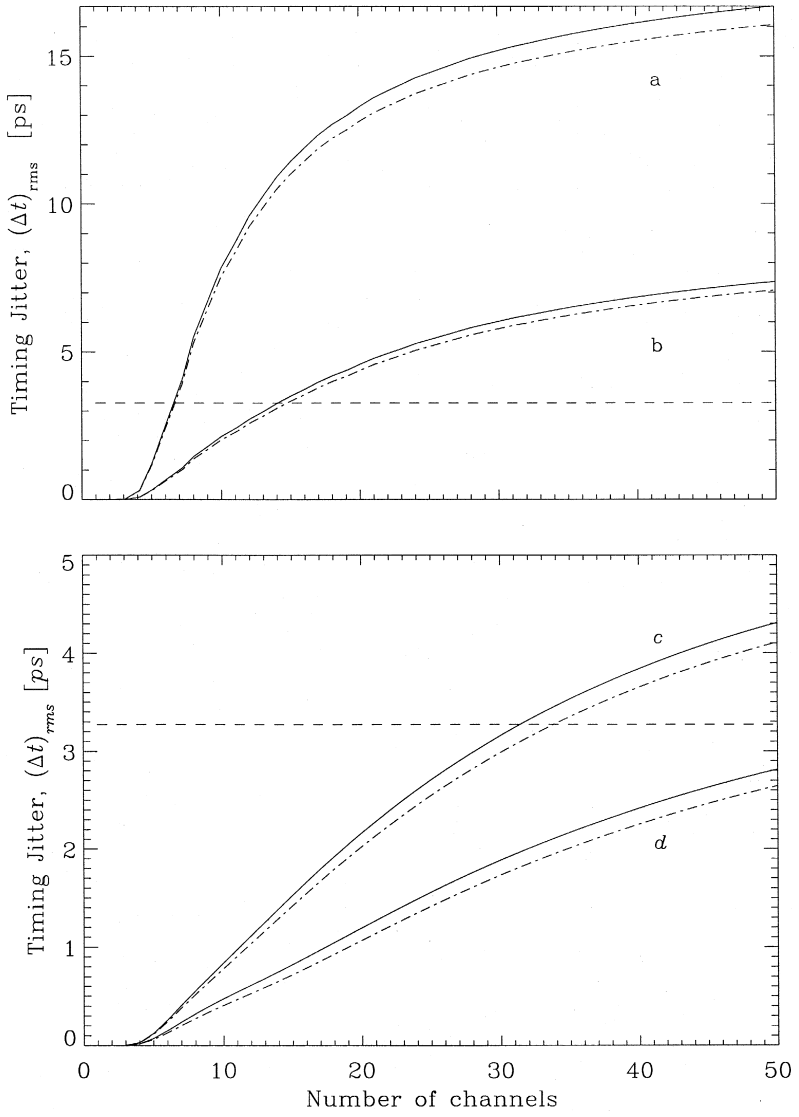


Fig. 5. The rms timing jitter of the outermost channel $J$ of a multi-channel WDM system at 10000 km vs the total number of channels with: (a) no dispersion management; (b) 2-step dispersion ($\theta = 0.5$); (c) 3-step dispersion map with equal step sizes; (d) 4-step dispersion map with equal step sizes. Solid curve: lumped filters; dot-dashed curve: distributed filters. The dashed line corresponds to the maximum $(\Delta t)_{\text{rms}} = 3.27\text{ps}$ allowed for BER $< 10^{-9}$ and system tolerance $r = 0.2$. System parameters are the same as in Fig. 1.

number of channels in the WDM system. We present our results for both the lumped model (solid lines) and the distributed model (dot-dashed lines) in the following situations: (a) no dispersion management; (b) 2-step dispersion map with fiber spans of equal length, i.e. $\theta = 0.5$; (c) 3-step dispersion map with equal step sizes; (d) 4-step dispersion map with equal step sizes. Fig. 5 demonstrates a significant reduction in the rms timing jitter for both models with increasing number of steps of the dispersion map. Here we consider a system tolerance of $r = 0.2$ which allows an rms timing jitter of 3.27 ps per channel (indicated by the horizontal line) in order that the BER be less than $10^{-9}$. Then with *either* filtering model, the maximum number of channels for error free transmission at 10 Mm with the specified system tolerance is 6 in the case of no dispersion management (Fig. 5a) and 15 in the case of 2-step dispersion map (Fig. 5b). For 3-step and 4-step dispersion management, a large number of 'error-free' channels are predicted by both models. The maximum number of channels allowed by the specified system tolerance for the lumped and distributed filtering models are (i) 31 and 33 with a 3-step dispersion map and (ii) 65 and 75 with a 4-step dispersion map respectively, with dispersion following the loss profile. We note that these numbers will increase significantly for both models with dispersion exactly compensating the loss profile.

The comparison between the system performances of a multi-channel transmission line with the lumped and distributed filter models in a fiber with a 2-step dispersion map is further exemplified in Fig. 6. Here we plot the maximum number of total channels $J_{\max}$

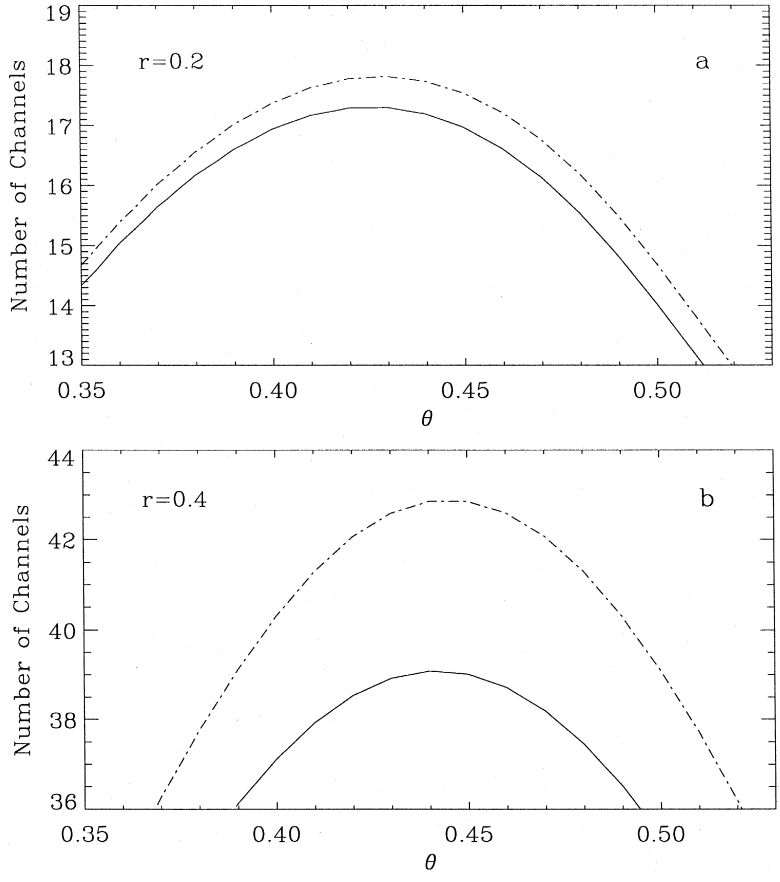


Fig. 6. The maximum number of channels for error-free (BER $< 10^{-9}$) transmission over 10000 km as a function of the parameter $\theta$ in a two-step dispersion map with system tolerance: (a) $r = 0.2$; (b) $r = 0.4$. Solid curve: lumped filters; dot-dashed curve: distributed filters.

estimated from Eq. (21) as a function of $\theta$ for: (i) lumped model (dot-dashed line); (ii) distributed model (solid line). We take $r = 0.2$ in Fig. 6a and $r = 0.4$ in Fig. 6b corresponding to maximum rms timing jitter per channel of 3.27 ps and 6.55 ps respectively, tolerated by the system. It is evident from Fig. 6 that the difference between the models is not significant. When $r = 0.2$, $J_{\max} = 16$ for the lumped model and $J_{\max} = 17$ for the distributed model (cf. Fig. 6a). In the case of $r = 0.4$, $J_{\max} = 38$ and 43 for the lumped and distributed models respectively (cf. Fig. 6b). Note that the maximum number of channels in both cases correspond to values of $\theta$ between 0.44 and 0.45. Therefore, the concept of 'optimal dispersion management' introduced in Ref. [6] remains valid independently of which filtering model is used.

However, it must be stressed that there are other important effects in a multi-channel communication system such as four-wave mixing and simultaneous collisions of solitons from more than two channels. Hence, the results presented in this section should be considered as a lower bound on the collision-induced timing jitter, and primarily indicative of the comparative role of the two filter models in a WDM system with dispersion following the loss profile.

## 5. Summary and conclusions

In this article a detailed analysis of collision induced timing jitter for a multi-soliton WDM system in presence of damping/amplification, filters and employing dispersion management where fiber dispersion approximates the loss/gain profile has been carried out. We have considered both lumped filters, when the filter is inserted at the amplifier locations, as well as distributed filter models. Our results indicate that for a wide range of system parameter values the predictions from the models are very close to each other.

First we considered two channel soliton WDM systems. When there is no dispersion management or for a 2-step dispersion map with fiber spans of equal length ($\theta = 0.5$) we found that the two models are extremely close (cf. Figs. 1a and 1b). There is a discrepancy between the models in the neighborhood of the value $\theta = 0.416$ which minimizes the first Fourier coefficient (cf. Figs. 1c and 2). However in this regime the values of timing jitter are extremely small and yield a negligible BER. With 3-step and 4-step maps the relative difference between the lumped and the distributed models is more evident. However in such cases the timing jitter is so small that (i) the absolute magnitude of the difference is small (cf. Fig. 3), and (ii) both models predict high numbers of 'error free' channels. It should be pointed out that when so many channels are admitted, other factors, such as third order dispersion, shock terms, Raman scattering, etc., that have not been considered in this discussion, must be taken into account. We also note that in all cases considered the timing jitter estimated from the distributed model was found to be somewhat lower than that is obtained from the lumped model.

Finally we remark that our values of timing jitter corresponding to multi-channel systems must be considered as indicative of the comparative information between the two filter models. In the multi-channel case we have only assumed pairwise interactions, as implied by leading order perturbation theory. With this assumption we are able to develop a multi-channel WDM timing jitter analysis in a straightforward way. However, other important and complex effects, outside the scope of the present work, such as residual four-wave mixing [26,29] and simultaneous collisions of more than two solitons [31] should be taken into account in order to have a more comprehensive and realistic theory of timing jitter.

## Acknowledgements

This effort was partially sponsored by the National Science Foundation under grant number ECS-9800152 and the Air Force Office of Scientific Research, Air Force Materials Command, USAF, under grant number F49620-97-1-0017.

## Appendix A. Lumped and distributed filter models

In a practical transmission line the action of filters is concentrated (or 'lumped') at discrete positions $z = nz_f$, along the fiber where $z_f = l_f/z_*$ and $l_f$ is

the filter spacing. The action of a filter on the pulse is described in the frequency domain by the relation

$$\hat{u}(z_f^+,\omega)=\hat{H}(\omega)\,\hat{u}(z_f^-,\omega), \tag{A.1}$$

where $\hat{H}(\omega)$ is the complex filter transfer function ($\hat{F}(\omega)$ represents the Fourier transform of a generic function $f(t)$). In the case of Fabry-Perot étalon filters, $\hat{H}(\omega)=(1-R)/(1-R\exp[i(\omega-\omega_f)2d/c])$, where $R$ is the reflectivity and $d$ is the mirror spacing and $\omega_f$ is the filter peak frequency (cf. Ref. [7]).

Note that Eq. (A.1) is the solution of the differential equation

$$\hat{u}_z=\left(\hat{H}(\omega)-1\right)\delta(z-z_f)\,\hat{u}$$

at $z=z_f^+$. Hence the lumped filtering effects along the fiber can be incorporated into Eq. (1) through the inverse Fourier transform of

$$\hat{F}(\omega,z)=\sum_{n=-\infty}^{\infty}\left(\hat{H}(\omega)-1\right)\delta(z-nz_f),$$

where the Dirac-delta functions are taken to act on the left, i.e., $\delta(z-z_f)u(z,t)=u(z_f^-,t)$. As is customary, we then expand $\hat{H}(\omega)-1$ in Taylor series in the neighborhood of the filter peak frequency $\omega=\omega_f$ and retain only the first few terms assuming $\omega$ is sufficiently close to $\omega_f$. The linear term corresponds to an unimportant time translation of the pulse, and the cubic term does not contribute to leading order in our analysis; so they are ignored. Therefore, keeping the relevant terms in the Taylor series expansion and converting to the time domain we get

$$F[t]_{\text{lumped}}=\left[\eta_0-\eta_2\left(i\partial_t-\omega_f\right)^2\right]z_f\times\sum_{n=-\infty}^{\infty}\delta(z-nz_f), \tag{A.2a}$$

where $\eta_2$ is the filter strength, $\eta_0$ is the additional gain required to overcome the energy loss due to filters, and $\eta_0 z_f,\eta_2 z_f$ are assumed to be small. Eq. (A.2a) constitutes the so-called 'lumped' filter model (cf. Ref. [5]). For convenience we introduce the quantity

$$\eta(z)=\eta_2 z_f\sum_{n=-\infty}^{\infty}\delta(z-nz_f), \tag{A.2b}$$

which will be useful when dealing with the lumped model. Note in Eq. (A.2b) the presence of the additional factor $z_f$ which is a useful normalization. As is commonly done, we will consider the filters to be positioned at amplifier locations, i.e., $z_f=z_a$.

In practice, the filter action is usually approximated by distributing the effects of the filter over an amplification period. Solving $\hat{u}_z=\hat{F}[\omega]\hat{u}$ over one amplification period and then comparing with the lumped value in Eq. (A.1) yields the function $\hat{F}[\omega]=(1/z_f)\ln\hat{H}(\omega)$ which is independent of $z$. This leads to the so-called 'distributed' filter model: (cf. Ref. [6])

$$F[t]_{\text{distributed}}=\eta_0-\eta_2\left(i\partial_t-\omega_f\right)^2. \tag{A.2c}$$

Throughout this work, we use the value $\eta_2=0.25$.

## Appendix B. Timing shifts in the lumped model

In this appendix we derive the relative timing shift for a two-soliton interaction in the case of lumped filtering. We start from (Eqs. (10)) and compute $a(z)$ first. In this case, $H(z)$ is the 'floor' function $H(z)=(4/3)\eta_2[z-s(z)]$, where $s(\zeta)$ is the periodic extension of $s(\zeta)=\zeta$, $0\le\zeta<z_f$, $z_f$ being the filter spacing which we take to be equal to $z_a$. Note that, since $\zeta(nz_a)=nz_a$, the function $H(z)$ has the *same* representation in both variables i.e.,

$$H(z(\zeta))=(4/3)\eta_2(z-s(z))=(4/3)\eta_2(\zeta-s(\zeta))=H(\zeta).$$

In order to compute $a(z)$, it is convenient to use the variable $\zeta$ instead of $z$ and evaluate the integral

$$a(z(\zeta))=\int_{\zeta}^{\infty}\exp[H(\zeta)-H(\zeta')]\,d\zeta',$$

which can be integrated after expanding $\exp[4\eta_2 s(\zeta)/3]$ in Fourier series. The result is

$$a(z(\zeta))=\exp[-4\eta_2 s(\zeta)/3]\times\sum_{m=-\infty}^{\infty}\frac{\sigma_m z_f\exp[2m\pi i\zeta/z_f]}{(4/3)\eta_2 z_f-2m\pi i}, \tag{B.1}$$

where

$$\sigma_m(\eta_2) = \frac{\exp[4\eta_2 z_f/3] - 1}{(4/3)\eta_2 z_f - 2m\pi i}$$

are the Fourier coefficients of $\exp[4\eta_2 s(\zeta)/3]$. The series on the right hand side of Eq. (B.1) can be explicitly summed:

$$\sum_{m=-\infty}^{\infty} \frac{\sigma_m z_f \exp[2m\pi i\zeta/z_f]}{(4/3)\eta_2 z_f - 2m\pi i} = \big(\alpha z_f - s(\zeta)\big)\exp[4\eta_2 s(\zeta)/3], \quad \text{(B.2)}$$

which yields the simple expression

$$a(z(\zeta)) = \alpha z_f - s(\zeta),$$

where $\alpha = 1/(1 - \exp[-4\eta_2 z_f/3])$. Eq. (B.2) is obtained by differentiating $\sigma_m$ with respect to $\eta_2$ which leads to

$$\sigma_m z_f/\big[(4/3)\eta_2 z_f - 2m\pi i\big] = \alpha z_f \sigma_m - (3/4)\,\partial\sigma_m/\partial\eta_2$$

and then noting that $\partial\sigma_m/\partial\eta_2$ are the Fourier coefficients of $\partial\big(\exp[4\eta_2 s(\zeta)/3]\big)/\partial\eta_2$. Then, after changing variable from $z$ to $\zeta$, the timing shift in Eqs. (10) can be expressed as

$$\delta t = -\int_{-\infty}^{\infty} \alpha z_f G(z(\zeta))\frac{d}{d\zeta} f(\zeta(z) - \zeta_o)\,d\zeta + \int_{-\infty}^{\infty} s(\zeta) G(z(\zeta))\frac{d}{d\zeta} f(\zeta(z) - \zeta_o)\,d\zeta.$$

Both integrals in the above expression for $\delta t$ can be evaluated by expanding $G(z(\zeta))$ and $s(\zeta)G(z(\zeta))$ in Fourier series and then integrating by parts together with the relation $d\zeta = D(z)dz$. The function $G(z(\zeta))$ in the first integral has period $z_a$, whereas $s(\zeta)G(z(\zeta))$ in the second integral has period $z_p$, defined as the lowest common period of $z_a$ and $z_f$ if $z_f \neq z_a$. Since we are considering the case where a filter is placed after each amplifier, we set $z_f = z_a = z_p$ and finally obtain

$$\delta t = \sum_{m=-\infty}^{\infty} (i/2)\, p_m\, c_m(\Omega)\exp[2m\pi i\zeta_o/z_a], \quad \text{(B.3)}$$

where $p_m = \alpha z_a G_m - S_m$ (cf. Eq. (13b)),

$$c_m(\Omega) = (4m\pi i/z_a)\int_{-\infty}^{\infty} f(\zeta)\, e^{2m\pi i\zeta/z_a} d\zeta = \pi^5 m^3/\Omega^4 z_a^3 \sinh^2\big(m\pi^2/2\Omega z_a\big), \quad \text{(B.4)}$$

$$S_m = (1/z_a)\int_0^{z_a} s(\zeta) G(z(\zeta)) \times \exp[-2m\pi i\zeta(z)/z_a]\,d\zeta \quad \text{(B.5)}$$

and the $G_m$ were defined in Eq. (15). Rearranging the right hand side of Eq. (B.3) as a sine Fourier series we obtain Eq. (11), which is the desired result.

## Appendix C. Timing shifts in the distributed model

In this appendix we present a detailed derivation of the collision-induced timing shifts in a fiber with stepwise dispersion approximating the fiber loss and with filtering effects distributed over an amplifier spacing. Like the lumped case as in Appendix A, we first evaluate $a(z)$ in Eqs. (10). The integral for $a(z)$ can be written as

$$a(z) = \int_0^{\infty} \exp[-4\eta_2 s/3] D(z+s)\,ds,$$

after a change of variable $z' = s + z$. Recall that in the distributed case $H(z) = (4/3)\eta_2 z$. Dividing the interval $(0,\infty)$ in steps of $z_a$ and using the fact that $D(z)$ is periodic over each step, the above integral can be expressed as an infinite sum:

$$a(z) = I(z)\sum_{n=0}^{\infty} \exp[-n(4\eta_2 z_a/3)] = \alpha I(z),$$

$$I(z) = \int_0^{z_a} \exp[-4\eta_2 z'/3] D(z+z')\,dz'$$

and $\alpha = 1/(1 - \exp[-4\eta_2 z_a/3])$. Note that in the above, $0 \le z' < z_a$. Since $a(z)$ is periodic, one can also restrict $z$ to one period $0 \le z < z_a$. Setting $u = z + z'$ and using the periodicity of $D(z)$, the integral $I(z)$ can be split as

$$I(z) = \exp[4\eta_2 z/3]\left[\int_z^{z_a} \exp[-4\eta_2 u/3] D(u)\, du + \int_0^z \exp[-4\eta_2 (u + z_a)/3] D(u)\, du\right]. \tag{C.1}$$

Each integral in Eq. (C.1) is then evaluated for stepwise dispersion management described in Section 2 by fixing $z$ in a given interval $z_{s-1} \le z < z_s$ and by taking $D(u) = D_r$, $z_{r-1} \le u < z_r$ where $D_r$ is given by Eq. (14). The resulting expression for $a(z)$ is

$$a(z) = \alpha I(z) = (3/4\eta_2)\left(D_s - \tilde{D}_s \exp[4\eta_2 z/3]\right), \quad z_{s-1} \le z \le z_s, \tag{C.2}$$

where $\tilde{D}_s$ is defined as

$$\tilde{D}_s = D_s X_s - \alpha\left[\sum_{j=s+1}^{S} K_j + e^{-(4/3)\eta_2 z_a} \sum_{j=1}^{s} K_j\right],$$

with $K_j = D_j(X_{j-1} - X_j)$ and $X_j = e^{-(4/3)\eta_2 z_j}$. Finally, the timing shift is obtained from Eqs. (10) after using $a(z)$ from Eq. (C.2)

$$\delta t = \int_{-\infty}^{\infty} a(z) G(z) \frac{d}{dz} f(\zeta(z) - \zeta_o)\, dz = \sum_{m=-\infty}^{\infty} (i/2)\, p_m\, c_m(\Omega) \exp[2m\pi i \zeta_o/z_a], \tag{C.3}$$

with $p_m = (3/4\eta_2)\hat{G}_m$ (cf. Eq. (13a)). The explicit form of $\hat{G}_m$ is given by

$$\hat{G}_m = (1/z_a)\int_0^{z_a}\left(D_s - \tilde{D}_s \exp[4\eta_2 z/3]\right) g(z) \times \exp[-2m\pi i \zeta(z)/z_a]\, dz = \sum_{s=1}^{S}\left[G_{m,s} D_s - \tilde{G}_{m,s}\tilde{D}_s\right],$$

with $G_{m,s} = G_{m,s}(\Gamma)$ (cf. Eq. (15)) and $\tilde{G}_{m,s} = G_{m,s}(\Gamma - 2\eta_2/3)$. Although the expression for $\hat{G}_m$ is fairly complicated, its numerical value differs from $G_m$ only by a term $O(z_a)$, which arises from the periodic oscillation of the local dispersion $D(z)$ about its mean $\bar{D} = 1$. Indeed, expressing $D(z)$ as $D(z) = 1 + \Delta(z)$ and evaluating the integral for $a(z)$ using the Fourier series for $\Delta(z)$ yields $a(z) = 3/4\eta_2 + O(z_a)$. Consequently in Eq. (C.3), $p_m = (3/4\eta_2)G_m + O(z_a)$ which is a small correction to the overall timing shift as we noted earlier in Section 2 (cf. Eq. (9)).

## References

[1] L.F. Mollenauer, P.V. Mamyshev, J. Quantum Electron. 34 (1998) 2089.
[2] S.K. Turitsyn, T. Schäfer, K.H. Spatschek, V.K. Mezenetsev, Opt. Commun. 163 (1999) 122.
[3] L.F. Mollenauer, S.G. Evangelides, J.P. Gordon, J. Lightwave Technol. 9 (1991) 362.
[4] R.B. Jenkins, J.R. Sauer, S. Chakravarty, M.J. Ablowitz, Opt. Lett. 20 (1995) 1964.
[5] A. Mecozzi, J. Opt. Soc. Am. B 13 (1998) 152.
[6] M.J. Ablowitz, G. Biondini, S. Chakravarty, R. Horne, Opt. Commun. 150 (1998) 305.
[7] E.A. Golovchenko, A.N. Pilipetskii, C.R. Menyuk, J.P. Gordon, L.F. Mollenauer, Opt. Lett. 20 (1995) 539.
[8] Y. Kodama, A. Hasegawa, Opt. Lett. 17 (1992) 31.
[9] Y. Kodama, S. Wabnitz, Opt. Commun. 113 (1995) 395.
[10] B.A. Malomed, Opt. Lett. 23 (1998) 1250.
[11] A. Mecozzi, H.A. Haus, Opt. Lett. 17 (1992) 988.
[12] A. Mecozzi, J.D. Moores, H.A. Haus, Y. Lai, Opt. Lett. 16 (1991) 1841.
[13] M. Midrio, P. Franco, F. Matera, M. Romagnoli, M. Settembre, Opt. Commun. 112 (1994) 283.
[14] L.F. Mollenauer, P.V. Mamyshev, J.P. Gordon, Opt. Lett. 24 (1999) 220.
[15] W. Forysiak, J.F.L. Devaney, N.J. Smith, N.J. Doran, Opt. Lett. 22 (1997) 600.
[16] E.A. Golovchenko, A.N. Pilipetskii, C.R. Menyuk, Opt. Lett. 22 (1997) 1156.
[17] A. Hasegawa, S. Kumar, Y. Kodama, Opt. Lett. 21 (1996) 39.
[18] T. Hirooka, A. Hasegawa, Opt. Lett. 23 (1999) 768.
[19] D.J. Kaup, B.A. Malomed, J. Yang, Opt. Lett. 23 (1998) 1600.
[20] B.A. Malomed, Opt. Commun. 147 (1998) 157.
[21] P.V. Mamyshev, L.F. Mollenauer, Opt. Lett. 24 (1999) 448.
[22] A.M. Niculae, W. Forysiak, A.J. Gloag, J.H.B. Nijhof, N.J. Doran, Opt. Lett. 23 (1998) 1354.
[23] H. Sugahara, H. Kato, Y. Kodama, Electron. Lett. 33 (1997) 1065.
[24] W. Forysiak, K.J. Blow, N.J. Doran, Electron. Lett. 29 (1993) 1225.

[25] M. Suzuki, I. Morita, N. Edgawa, S. Yamamoto, H. Taga, S. Akiba, Electron. Lett. 31 (1995) 2027.
[26] P.V. Mamyshev, L.F. Mollenauer, Opt. Lett. 21 (1996) 396.
[27] L.F. Mollenauer, P.V. Mamyshev, M.J. Neubelt, Electron. Lett. 32 (1996) 471.
[28] M. Nakazawa, K. Suzuki, H. Kubota, A. Sahara, E. Yamada, Electron. Lett. 34 (1998) 103.
[29] M.J. Ablowitz, G. Biondini, S. Chakravarty, R.B. Jenkins, J.R. Sauer, J. Opt. Soc. Am. B 14 (1997) 1788.
[30] S. Chakravarty, M.J. Ablowitz, J.R. Sauer, R.B. Jenkins, Opt. Lett. 20 (1995) 136.
[31] S.G. Evangelides, J.P. Gordon, J. Lightwave Technol. 14 (1996) 1639.